JOURNAL OF CATALYSIS 96, 347–356 (1985)

Paraffin Isomerization Catalyzed by Polymer-Supported Superacids

K. M. DOOLEY*,† AND B. C. GATES*

*Center for Catalytic Science and Technology, Department of Chemical Engineering, University of Delaware, Newark, Delaware 19716; and †Department of Chemical Engineering, Louisiana State University, Baton Rouge, Louisiana 70803

Received September 25, 1984; revised June 26, 1985

Solid superacids were prepared by the reaction of metal-halide Lewis acids with macroporous sulfonated poly(styrene-divinylbenzene), and a supported trifluoromethanesulfonic acid was prepared on the unsulfonated support. These polymers were used to catalyze the isomerization and dehydrogenation of *n*-butane in a flow reactor at 60–120°C and 0.54 bar butane partial pressure. The catalysts were active in the presence of small amounts of HCl co-catalyst (the reaction rates being about 2×10^{-9} mol/g · s for the most active catalysts), but rapid deactivation resulted from loss of hydrogen halide. Catalysts prepared from $SnCl_4$ and $TiCl_4$ were relatively inactive in comparison with those prepared from SbF_5 and BF_3; the catalysts prepared from $AlCl_3$ were as active as those containing fluorine and more stable. The activities of the catalysts are compared to the acid strengths of unsupported conjugate Lewis-acid analogs indicated by the Hammett acidity function. © 1985 Academic Press, Inc.

INTRODUCTION

The acid-catalyzed reactions of C_4–C_6 hydrocarbons have become increasingly important for boosting motor fuel octane numbers by isomerization or alkylation. The trend has been toward use of more active catalysts, since low temperatures favor equilibrium conversions to the desired branched isomers and alkylation products. Hydroisomerization catalysts are employed in today's processes, namely, Pt-containing chlorided aluminas and Pt/$AlCl_3$-containing aluminas, which are used for both *n*-butane and C_5–C_6 mixtures (*1*). These catalysts are sensitive to impurities such as sulfur and water, but they are far less susceptible than the previously used supported $AlCl_3$ catalysts to deactivation resulting from dehalogenation and conjunct polymerization of olefins (*2*). However, the hydroisomerization processes require hydrogen partial pressures up to 100 bar and temperatures of 100–200°C.

Catalysis of paraffin isomerization can be effected with very strong acids alone, and the development of superacids (proton donors stronger than pure H_2SO_4) has provided new opportunities for low-temperature conversions. Superacids are typically formed by combining a Brønsted acid with a strong Lewis acid. A solvolysis reaction may take place, producing an acid halide, depending upon the reaction conditions (*3–5*). Another product of the synthesis, a Lewis–Brønsted acid pair, acts upon neighboring Brønsted acid species to create and stabilize the superacidic proton donor, e.g., H_2F^+. This chemistry is well documented for superacid solutions containing $FSO_3H + SbF_5$ and $HF + SbF_5$ (*4, 6*). Spectroscopic evidence indicates that such superacids are capable of protonating aromatic hydrocarbons and paraffins at low temperatures, thereby initiating a variety of catalytic reactions (*7, 8*).

Superacids initiate the isomerization and disproportionation reactions of even very pure straight-chain C_4–C_6 paraffins, but the soluble catalysts easily undergo hydrolysis, reduction, and oxygenation (*9–12*). Some reactions leading to catalyst deactivation include the following (M = metal, X = halogen):

0021-9517/85 $3.00

$$HX \cdot MX_n + H_2O \rightarrow HX \cdot MX_{n-1}OH + HX \tag{1}$$

$$MX_5 + H_2O \rightarrow MX_3 + 2HX \tag{2}$$

$$MX_n + \tfrac{1}{2}O_2 \rightarrow MOX_{n-2} + X_2 \tag{3}$$

Superacids on supports offer the potential advantage of easier isolation from H_2O and O_2 by allowing the use of a gas-phase reactant stream; they are also less corrosive than the superacid solutions. Some supported superacid catalysts are listed in Table 1 with representative reactions. As the mild reaction conditions suggest, these superacids have extremely high catalytic activities for paraffin conversions, and many Brønsted–Lewis acid combinations appear to be supported without the miscibility problems so common in comparable homogeneous systems. There is only little information in the literature, however, concerning the stabilities of these catalysts.

The few systematic investigations of solid superacid catalysts include those of Fuentes *et al.* (*13*), who used aluminum chloride/sulfonated polymer and aluminum chloride/silica catalysts, and Hattori *et al.* (*14*), who used SbF_5 on sulfonated or fluorided metal oxides. These investigators showed that catalyst supports with widely different Brønsted acid strengths, when combined with the same Lewis acid, give supported superacids with roughly the same catalytic properties.

In both of these investigations, it was observed that there was persistent catalyst deactivation that was seemingly only slightly dependent on the combination of Brønsted and Lewis acids. Fuentes *et al.* (*13*) found that activity could be maintained only by continuous addition of acid halide to the reactant stream.

The objectives of the present work were to provide a broader systematic investigation of supported superacid catalysts and, in particular, to determine the effect of Lewis acids of various strengths on catalytic activity and characterize the catalyst deactivation. The catalysts were prepared from several Lewis acids ($AlCl_3$, $SnCl_4$, $TiCl_4$, SbF_5, and BF_3) and sulfonated macroporous poly(styrene-divinylbenzene) supports. A catalyst was also prepared by adsorbing trifluoromethanesulfonic acid onto an unsulfonated macroporous poly (styrene-divinylbenzene). The catalysts were characterized by their activities for *n*-butane isomerization at 60–120°C.

TABLE 1

Solid Superacid Catalysts Used for Hydrocarbon Conversions

Solid acid catalyst	Support(s)	Reaction(s)	Reaction conditions	Characterization of acid sites	Ref.
$SbF_5/CF_3(CF_2)_xSO_3H$	CaF_2, polytetrafluoroethylene, AlF_3	C_5 isomerization	≈50°C	x = 1–7; Lewis : Brønsted acid ratio = 1 : 3	(*29*)
SbF_5,PF_5,BF_3/HF,HCl, FSO_3H,CF_3SO_3H	Fluorinated graphite	C_4–C_8 isomerization, propylene–C_4 alkylation	30–150°C, 1–10 bar 0–150°C, 1–30 bar	Lewis : Brønsted acid ratio = 0.2 : 1.0	(*30*)
SbF_5,TaF_5/HF	Fluorided or sulfonated Al_2O_3	C_4–C_5 isomerization	50°C, 1–15 bar		(*19*)
$AlCl_3$,$AlCl_3/–SO_3H$	SiO_2, poly(styrene-DVB)	C_4 isomerization disproportionation	20–100°C, 1 bar	Cl : Al = 1 : 2	(*21*)
SbF_5/FSO_3H	Fluorided SiO_2–Al_2O_3, SiO_2, Al_2O_3, etc.	C_4 isomerization, disproportionation	>300°C	≈17 wt% Sb	(*14*)
$BF_3/–SO_3H$	Poly(styrene-DVB)	Olefin–alkane isomerization	(−20)–60°C, 10–30 bar	Lewis : Brønsted acid ratio > 2	(*31*)

TABLE 2

Properties of Poly(Styrene-Divinylbenzene) Catalyst Supports

Polymer	$-SO_3H$ group content (meq/g)	Surface area (m^2/g)	Percentage crosslinking (wt% divinylbenzene)	Macropore void fraction	Maropore average equivalent diameter (nm)	Microparticle average diameter (nm)
Amberlyst 15	4.4–4.8	45–55	20	0.32–0.36	20–40	70–90
Amberlyst XN-1010	3.3–3.6	540–600	80	0.47–0.50	4–5	7–8
XAD-2	0.0	300	20	0.42	9	—

EXPERIMENTAL METHODS

The polymer supports were macroporous sulfonated poly(styrene-divinylbenzene) (Amberlyst 15 and Amberlyst XN-1010, Rohm & Haas) and a similar macroporous polymer which was unsulfonated (Amberlite XAD-2, Rohm & Haas). Physical properties of these supports are summarized in Table 2.

The resins were brought in contact with $AlCl_3$, $SnCl_4$, $TiCl_4$, SbF_5, BF_3, or CF_3SO_3H according to procedures described elsewhere (*15*, *16*). The synthesis conditions were as follows: temperature, 0–150°C; total pressure, 1 bar; reaction time, 12–240 h. Purified N_2 was used to blanket the reaction mixtures. The resulting catalysts were analyzed for metal and, in some cases, halogen and sulfur (Schwarzkopf Microanalytical Laboratory, Woodside, N.Y.).

The catalysts were handled under dry N_2 to minimize contamination by water; samples were loaded into stainless-steel flow microreactors under N_2 and brought onstream with minimal contamination.

The reactant stream flowing to the catalytic reactor typically consisted of 45 mol% *n*-butane (research grade, Phillips, >99.9%), 10 mol% HCl (electronic grade, Matheson, >99.99% and <30 ppm water), and 45 mol% He (ultrahigh purity, Matheson, >99.99%). The He and *n*-butane were dried by passage through molecular sieve traps, but the HCl was used as received. The flow rates were regulated with mass flow controllers (Brooks Model 8750).

The vertical upflow tubular reactor was 24 cm long and 1.27 cm o.d. It was encased in an insulated aluminum heating block containing constant-load resistance heaters. The reactor temperature was measured with a thermocouple embedded in the reactor wall at the position of the catalyst bed; it was controlled to ±0.5°C by means of a time-proportioning PI controller (Thermo-Electric).

The feed and product streams were analyzed with an on-line gas chromatograph (Antek Model 300) equipped with a flame ionization detector. A single-loop (0.25 cm^3), six-port sampling valve (Valco) was used to introduce the samples into a 2.24-mm-long, 0.318-cm.-o.d. *n*-octane/Porasil C column (60–80 mesh, Waters), which was held for 7 min at 35°C, then ramped at 10°C/min to 110°C and held for 4 min at 110°C. Additional samples were collected in a trap held in an acetone–dry ice bath and analyzed with a gas chromatograph–mass spectrometer (Hewlett–Packard, Models 5750 and 5930).

In a typical experiment, the reactor was fed with HCl in He for 1 h at the desired temperature. Then the *n*-butane flow was started and sampling commenced. Samples were taken every 20 min; in most experiments, at least four samples were taken under a given set of conditions.

TABLE 3

Quantitative Microanalysis of Resin Samples

Sample No.	Support	Halogen-containing acid	Analysis (wt%)			Atomic ratio	
			Metal	Halogen	Sulfur	Halogen : metal	Sulfur : metal
1	Amberlyst 15	$AlCl_3$	3.3	[a]	[a]	[a]	[a]
2	Amberlyst 15	$AlCl_3$	0.55	0.52	18.5	0.71	28
3	Amberlyst 15	$AlCl_3$	0.011	0.017	16.28	1.2	1200
4	XN-1010	$AlCl_3$	4.6	[a]	[a]	[a]	[a]
5	XN-1010	$AlCl_3$	0.21	[a]	[a]	[a]	[a]
6	XN-1010	$AlCl_3$	0.080	0.041	11.64	0.39	120
7	Amberlyst 15	[b]	2.0	[a]	[a]	[a]	[a]
8	Amberlyst 15	$TiCl_4$	4.16	3.96	10.57	1.3	3.8
9	XN-1010	$TiCl_4$	2.66	1.49	10.42	0.76	5.9
10	Amberlyst 15	$SnCl_4$	2.96	1.58	15.29	1.8	19
11	Amberlyst 15	$SnCl_4$	2.30	0.22	16.10	0.32	26
12	XN-1010	$SnCl_4$	5.44	4.33	9.76	2.7	6.7
13	Amberlyst 15	SbF_5	2.19	[a]	[a]	[a]	[a]
14	Amberlyst 15	BF_3	1.34	[a]	[a]	[a]	[a]
15	XAD-2	CF_3SO_3H	[c]	12.29	7.08	2.92	1.0

[a] Not determined.

[b] Ion exchanged with Al^{3+}.

[c] This sample was found to contain 2.3 meq/g acid groups by titration of total acidity.

Experiments were also performed to determine the effect of olefin in the feed on the rate of catalytic reaction. In one set of experiments, a helium feed stream containing 1.7% total butenes was introduced as a pulse into the steadily flowing feed stream containing 45 mol% *n*-butane, 45 mol% helium, and 10 mol% HCl. The pulse, with a duration of 1 min, was injected at the beginning of the experiment, and the pulse and steady feed streams were mixed in a 1 : 3.5 ratio by volume. In the other experiments, the same butene–helium mixture was substituted for the usual helium carrier gas stream. The *n*-butane and HCl streams were unchanged, as were all other operating conditions.

Further details of the experiments are available in a thesis (*16*).

RESULTS

The microanalytical results for the catalysts are given in Table 3. The resins prepared with $AlCl_3$ had widely varying aluminum contents, as a consequence of the variation of the temperature of contacting of the $AlCl_3$ with the resin. At temperatures ≥130°C, high aluminum contents were observed, but at temperatures <110°C, almost Al-free resins were obtained.

All the catalysts were found to be active for the isomerization and dehydrogenation of *n*-butane at 60–120°C. The observed products, in order of decreasing yield, were isobutane, butenes (all isomers), propane, the pentane isomers, and traces of higher molecular weight products.

When HCl was not present in the feed, the resins rapidly lost activity, becoming almost inactive within 1 h on stream (which corresponds to less than 0.01 turnovers, based on the total number of acid sites). When these same catalysts were pretreated by heating overnight in N_2 at 1 Torr and 100°C, the adsorbed HCl was removed and the catalysts were inactive even initially (*15, 16*). Additional experiments were done confirming the necessity of the adsorbed acid halide for catalytic activity; the results are summarized elsewhere (*13, 15, 16*).

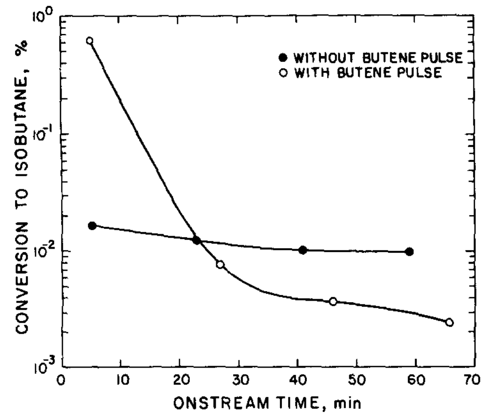

FIG. 1. Acceleration of *n*-butane isomerization by butenes. A pulse of 1.7 mol% total butenes (in helium) was injected at time zero into a stream of (by vol) *n*-butane, 0.45; helium, 0.45; HCl, 0.10. The total flow rate was 49 cm³/min. Reaction was carried out at 60°C and 0.54 bar butane partial pressure with catalyst sample 4 ($AlCl_3$/XN-1010, 4.6 wt% Al, 0.51 g). The pulse duration was 1 min.

The results of the experiments in which butenes were incorporated in the feed are presented in Figs. 1 and 2. The effect of butene pulses on conversion of *n*-butane to isobutane is shown in Fig. 1. The effect of continuous addition of small quantities of butenes is shown in Fig. 2. The effects of butene were similar in the two sets of experiments: the initial rate of isomerization of *n*-butane was at least an order of magnitude higher with the butene initiator present, but it rapidly declined with time onstream, returning to about the value observed with no initiator present.

Initial rates of butane isomerization were typically obtained from experiments with feeds including HCl but no more than traces of olefins. Typical results are shown in Fig. 3; a second-order polynomial curve-fit was used to extrapolate the data to time zero to determine the initial conversion; these data were used to calculate rates at time zero on the basis of the assumption that the conversions were differential (*16*).

Data are shown in Fig. 4 relating the isomerization rate at 60°C to the loading of aluminum chloride on the catalyst. The activity increased with increased loading of aluminum chloride, apparently reaching a saturation value for each support. The XN-1010-supported catalysts are more active than the Amberlyst 15-supported catalysts, which is explained by their higher surface areas (Table 2) and higher dispersions of the Lewis acid [as confirmed by transmission electron microscopy (*15*, *16*)].

DISCUSSION

The surfaces of the polymer catalysts incorporated pendant sulfonic acid and oxyhalide sulfonate groups, as well as aggregates inferred to be metal oxyhalides (*15*, *16*). Acid halides were strongly adsorbed on these surfaces; some acid halides were present as products of the catalyst synthesis reactions.

A pure *n*-butane feed is highly unreactive at temperatures <200°C, but it is reactive in the presence of a superacid catalyst (*3*, *14*–*19*). Such a catalyst was formed by the continuous flow of HCl, at 0.12 bar partial pressure, over the sulfonated metal oxyhalide polymers. Each component of this catalyst (sulfonate group, adsorbed HCl, and metal oxyhalide, either bound to or in close proximity to sulfonate groups) is essential, as

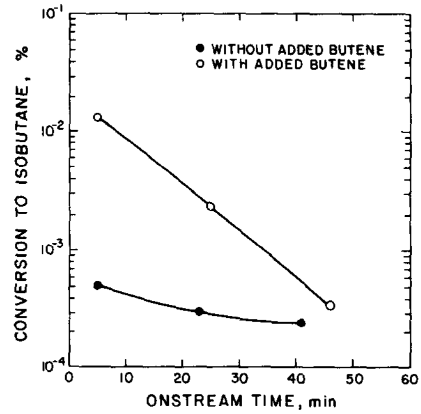

FIG. 2. Effect of continuous addition of 1.7 mol% total butenes (in helium) on the conversion of *n*-butane to isobutane catalyzed by sample 8 ($TiCl_4$/Amberlyst 15, 4.6% Ti, 1.54 g) at 60°C and 0.54 bar butane partial pressure. The feed flow rate was 49 cm³/min and the composition (by vol) was *n*-butane, 0.45; helium, 0.44; HCl, 0.10; butenes, 0.01.

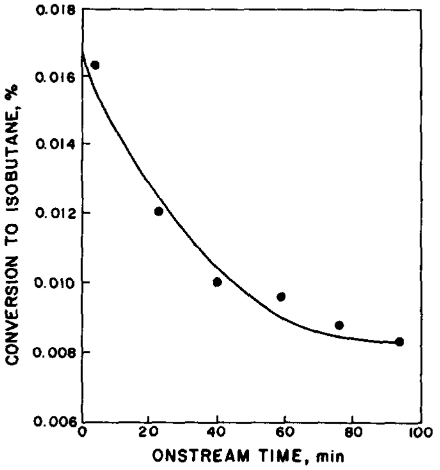

FIG. 3. Catalyst deactivation during n-butane isomerization at 60°C and 0.54 bar butane partial pressure. The catalyst was sample 5 ($AlCl_3$/XN-1010, 0.21 wt% Al, 1.26 g). The feed flow rate was 49 cm^3/min and the composition (by vol) was n-butane, 0.45; helium, 0.45; HCl, 0.10. The curve represents the second-order polynomial curve-fit to the data.

was demonstrated by n-butane isomerization experiments. The following preparations showed no measurable catalytic activity [rate $< 10^{-11}$ mol/(g of catalyst · s)]: (1) Amberlyst 15 resin in either H^+ or Al^{3+} form; (2) $AlCl_3$ sublimed onto an unsulfonated resin (in all other respects similar to Amberlyst 15); (3) this same Al-containing resin with added HCl; and (4) a physical mixture of p-toluenesulfonic acid and $AlCl_3$.

The isomerization rates determined from differential conversions of n-butane are inferred to be intrinsic catalytic reaction rates. The absence of significant intraparticle concentration and temperature gradients was confirmed by standard estimation procedures (*16*).

The isomerization rates determined with the stronger superacids [10^{-9} mol/(g of catalyst · s)] are comparable to those measured with aluminum chloride supported on silica and on sulfonated polymers under similar conditions (*13, 17, 18*). All these catalysts had approximately the same Cl : Al ratio (1 : 1, Table 3). Catalysts with 2 : 1 Cl : Al ratios were an order of magnitude more active under similar conditions (*13, 18*). SbF_5-impregnated metal oxides apparently showed even higher activities (*14, 19*); a summary of the activities obtained in this work and in comparable investigations is presented in Table 4; some of the data were interpolated linearly to provide comparisons at a common n-butane partial pressure of 0.54 bar.

We speculate that the high activities of the SbF_5-impregnated metal oxides were enhanced by higher olefin concentrations in the reactant feed stream. The data of Figs. 1 and 2 show that the initial isomerization rates are strongly dependent on the concentration of olefin impurity. At temperatures higher than 60°C, these impregnated oxides rapidly lost activity (*14*), probably, we suggest, because HF elimination reduced their halogen-to-metal ratios to values more characteristic of this work.

Since catalysts synthesized with low halogen-to-metal ratios were shown to be relatively low in activity, we infer that the observed losses of catalytic activity during operation were (at least in part) a result of halogen loss (e.g., by acid halide elimination). Temperature-programmed desorption experiments with an inert carrier gas confirmed that both halocarbon and acid

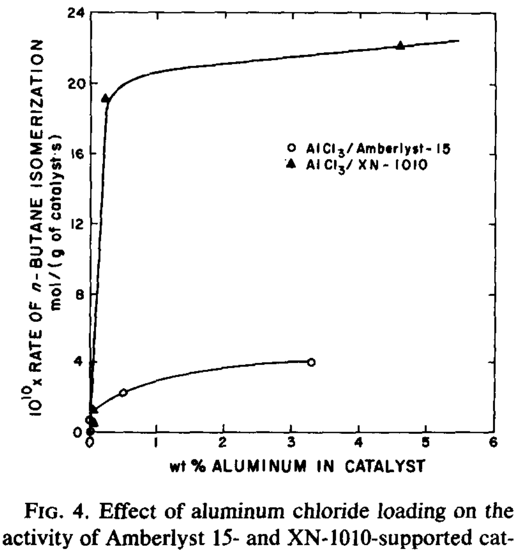

FIG. 4. Effect of aluminum chloride loading on the activity of Amberlyst 15- and XN-1010-supported catalysts, for isomerization of n-butane at 60°C and 0.54 bar butane partial pressure. The rates are initial rates, calculated as described in the text.

TABLE 4

Activities of Superacid Catalysts

Sample No.	Catalyst	Metal loading (wt%)	Halogen-to-metal molar ratio	*n*-Butane isomerization rate[a] (mol/g · s)	Ref.
—	$SbF_5/TiO_2–ZrO_2$	17	—	8.2×10^{-5}[b]	(*14*)
—	SbF_5/MgO	17	—	5.0×10^{-5}[b]	(*14*)
—	$SbF_5/SiO_2–Al_2O_3$	17	—	1.1×10^{-5}[b]	(*32*)
—	SbF_5/LaY	17	—	1.5×10^{-6}[b]	(*14*)
—	$SbF_5/Al_2O_3 + SO_2$	15	—	1.2×10^{-6}[b]	(*19*)
—	$SbF_5/Al_2O_3–B_2O_3$	10	—	3.6×10^{-7}[b]	(*19*)
—	$AlCl_3$/Amberlyst 15	5–7	2 : 1	9.9×10^{-8}	(*13*)
—	$AlCl_3/SiO_2$	4	1 : 1	2.3×10^{-9}	(*13*)
5	$AlCl_3$/XN-1010	0.21	1 : 1	1.9×10^{-9}	This work
13	SbF_5/Amberlyst 15	2.2	—	1.8×10^{-9}	This work
8	$TiCl_4$/Amberlyst 15	4.2	1 : 1	4.9×10^{-11}	This work

[a] Determined at 60°C and 0.54 bar.

[b] Interpolated value.

halide losses occurred at temperatures <150°C (*15*). We suggest that dehalogenation reactions typically cause the gradual deactivation of these supported superacids.

Initial rate data are shown in Tables 5 and 6 as a function of temperature for several of the catalysts. These data do not exhibit a typical Arrhenius dependence. The rates observed with catalysts prepared from $AlCl_3$ (Table 5) became independent of loading at the higher temperatures. The rates observed with catalysts prepared from SbF_5 or CF_3SO_3H (Table 6) show sharp decreases in isomerization activity as the temperature was increased beyond 60–80°C. These results suggest that active components were lost from these fluorine-containing catalysts at higher temperatures. The decrease in isomerization activity with increasing temperature is similar to that observed with SbF_5-impregnated metal oxide catalysts (*14*). Instability of these fluorine-containing catalysts is further suggested by the rapid decrease of conversion with time onstream shown by the data of Fig. 5 [cf. the data for a more stable aluminum chloride-containing catalyst (Fig. 3)]. The Amberlyst 15 having a high loading of aluminum chloride (3.3 wt% Al) was the most stable catalyst tested. It corresponds in structure and metal loading to the samples examined by Fuentes *et al.* (*13*), whose results indicated similar stability.

The dependence of rate on temperature shown in Tables 5 and 6 is consistent with the above hypothesis regarding deactivation; operation at the higher temperatures (>100°C) resulted in more rapid halogen losses and catalyst deactivation, and therefore lower observed activities. This effect is especially pronounced for the fluorine-containing catalysts (Table 6). Since HCl in He was allowed to flow over the catalyst for 1 h at the beginning of an experiment, there were undoubtedly surface rearrangements resulting in halogen losses even before the *n*-butane came in contact with the catalyst.

Characterization of the catalysts reported earlier (*15, 16*) suggests that the following reaction was occurring (written for an Al-containing catalyst, Ⓟ = polymer):

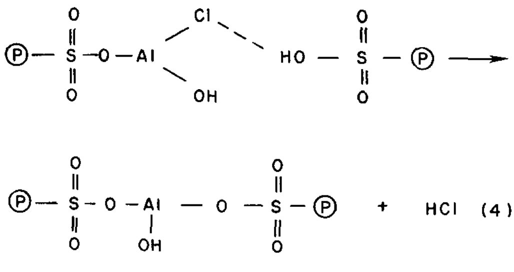

(4)

TABLE 5

Activities of Superacid Catalysts Prepared from $AlCl_3$

Sample No.	Catalyst	Metal loading (wt%)	Temperature (°C)	Isomerization rate[a] (mol/g · s)
1	$AlCl_3$/Amberlyst 15	3.3	60	4.1×10^{-10}
			80	5.3×10^{-10}
			120	8.7×10^{-10}
2	$AlCl_3$/Amberlyst 15	0.55	60	2.1×10^{-10}
			80	1.1×10^{-9}
			100	1.1×10^{-9}
5	$AlCl_3$/XN-1010	0.21	60	1.9×10^{-9}
			80	1.7×10^{-9}
			100	8.9×10^{-10}
			120	1.1×10^{-9}
6	$AlCl_3$/XN-1010	0.080	60	4.8×10^{-11}
			80	7.5×10^{-11}
			100	2.9×10^{-10}

[a] Determined at 0.54 bar.

Other dehalogenation pathways could also have been important, as suggested by reactions (1)–(3) (involving impurities or generated H_2) and the formation of halocarbons observed in TPD experiments.

Conjunct polymerization giving heavy aromatic products is excluded as a major cause of the deactivation for the following reasons: (1) the conversions were extremely low, and aromatic precursors such as the C_8 dimer were present only in trace amounts; (2) pentane and propane disproportionation products were also present in negligible amounts; the adsorbed C_8 dimer is an intermediate in disproportionation as well, as follows (*2*, *18*):

$$(CH_3)_3C^+ + C_4H_8 \rightarrow (CH_3)_3CHCH_2\overset{+}{C}HCH_2CH_3 \xrightarrow{\text{(several steps)}} C_5H_{10} + CH_3\overset{+}{C}HCH_3 \tag{5}$$

The relatively large amounts of butenes obtained from *n*-butane (as much as the primary product isobutane in some instances) suggest that the adsorbed butyl cation concentration was too small to drive reaction (5). A similar product distribution, with high yields of butenes and low yields of disproportionation products, has been observed for low conversions of butane catalyzed by amorphous Brønsted solid acids (*20*) and Lewis-acid-impregnated metal oxides (*21*).

The dependence of the catalytic activity on acid strength is not easily determined, because the sulfonated ion-exchange resins strongly adsorb even weak base indicators such as diphenylmethanol ($pK_a = -13.3$). For example, 0.20 g of Amberlyst 15 resin suspended in a 0.005 *M* solution of diphenylmethanol in *n*-octane at 25°C adsorbed 13% of the indicator (based on absorbance measurements at $\lambda_{max} = 258$ nm). The su-

TABLE 6

Activities of Superacid Catalysts Prepared from SbF_5 or CF_3SO_3H

Sample No.	Catalyst	Temperature (°C)	Isomerization rate[a] (mol/g · s)
13	SbF_5/Amberlyst 15	60	1.8×10^{-9}
		80	5.8×10^{-10}
		100	2.0×10^{-10}
		120	1.8×10^{-10}
15	CF_3SO_3H/XAD-2	60	7.4×10^{-10}
		80	1.7×10^{-9}
		100	3.8×10^{-10}
		120	5.1×10^{-10}

[a] Determined at 0.54 bar.

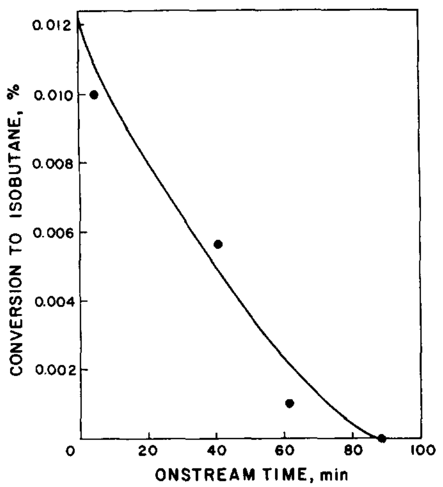

FIG. 5. Catalyst deactivation during *n*-butane isomerization at 60°C and 0.54 bar butane partial pressure. The catalyst was sample 13 (SbF_5/Amberlyst 15, 2.19 wt% Sb, 0.90 g). The feed flow rate was 49 cm^3/min and the composition (by vol) was *n*-butane, 0.45; helium, 0.45; HCl, 0.10. The curve represents the second-order polynomial curve-fit to the data.

peracid resins adsorbed diphenylmethanol even more strongly, but these data were widely scattered and seemingly dependent upon catalyst surface area, which in turn is a strong function of metal loading, halogen-to-metal ratio, etc. Therefore, it is impossible to relate these data to actual acid strengths in any meaningful way.

Our interest, however, lies in how our catalyst preparations qualitatively affect the acid strengths of sulfonated resins. With this purpose in mind, we examined whether a relation existed between the relative isomerization activity of a family of catalysts derived from Amberlyst 15, or its unsulfonated equivalent, and the Hammett acidities in solution of a typical Brønsted conjugate acid of the Lewis acid. These conjugate acid strengths are somewhat base-dependent; and they have been determined for the Lewis acids paired with Brønsted acids such as HF and HCl and also for the Lewis acids paired with water (*22*). We have used these latter literature values (*23–27*) for the case of proton donation to standard weak-base indicators. In most instances these measurements included a determination of acid strength under conditions of "almost pure" Lewis acid, i.e., the acid purified of all but traces of the proton donor; we have used these values preferentially.

Table 7 gives the relative isomerization activities for the Amberlyst 15-derived catalyst family along with the corresponding values of the Hammett acidity function (H_0) of the conjugate acid analogs in solution. It is suggested that the relative values of H_0 provide a first approximation to relative catalyst acid strengths, since our earlier characterization experiments indicated that the Lewis acids did not decompose upon reaction with the polymers (*13, 15–18*). We caution that these H_0 values are not the true values of the Hammett acidity function of the surface species; the data of Table 7 indicate, however, that the relative ordering of these conjugate acid H_0 values does provide a rough indication of the relative ordering of the acid strengths of the catalysts, as reflected in the relative isomerization rates. Because stronger Lewis acids give more active superacid catalysts, the supported Lewis acid is the key component in a solid superacid that includes both Lewis and Brønsted acid groups. The data also suggest that a threshold acid strength is necessary for initiation of acid-catalyzed reactions of a pure paraffin such as *n*-butane. The supported Ti and Sn halide catalysts evidently lack sufficient acid strength.

Beyond the threshold acid strength, the proton-donating ability of the catalyst seems not to be the only determinant of activity, which suggests that hydride transfer or carbenium ion rearrangement steps (which presumably are less dependent on the proton-donor strenght) may be rate limiting. A similar lack of dependence of catalytic activity on acid strength beyond a threshold has also been observed for hydrocarbon alkylation and isomerization catalyzed by superacids (at a similar range of H_0 values) in solution (*8, 28*).

Taken together, the data showing activity

TABLE 7

Relative *n*-Butane Isomerization Activities of Solid Superacid Catalysts, and the Hammett Acidity Functions of Analogous Conjugate Lewis Acid Precursors

Sample No.	Catalyst	Metal loading (wt%)	Relative activity[a]	$-H_0$
13	SbF_5/Amberlyst 15	2.19	1.0	15
15	CF_3SO_3H/XAD-2	[b]	0.41	14
1	$AlCl_3$/Amberlyst 15	3.3	0.23	13.5
2	$AlCl_3$/Amberlyst 15	0.55	0.12	13.5
14	BF_3/Amberlyst 15	1.34	0.15	11.4
8	$TiCl_4$/Amberlyst 15	4.16	0.027	7
10	$SnCl_4$/Amberlyst 15	2.96	0.00	7

[a] At 60°C, the initial isomerization rate divided by the corresponding rate for the most active catalyst.

[b] This sample was found to contain 2.3 meq/g acid groups by titration of total acidity.

as a function of metal loading and of acid strength (combined with the catalyst deactivation results) indicate that the next steps in research on solid superacids for paraffin conversion might be best directed to stabilization of the superacidic sites against loss of acid halide—which results in catalyst deactivation—rather than investigation of catalysts having higher acid strengths or higher concentrations of superacidic sites.

ACKNOWLEDGMENTS

We thank Professor G. C. A. Schuit for many helpful discussions. One of the authors (K.M.D.) acknowledges the support of the Shell Foundation in a Career Initiation Grant.

REFERENCES

1. Asselin, G. F., Bloch, H. S., Donaldson, G. R., Haensel, V., and Pollitzer, E. L., *Prepr. Div. Pet. Chem. Amer. Chem. Soc.* **17,** B4 (1972).
2. Condon, F. E., *in* "Catalysis" (P. H. Emmett, Ed.), Vol. VI, Chap. 2. Reinhold, New York, 1958.
3. Schmerling, L., and Ipatieff, V. N., U.S. Patent 2,369,691 (1945).
4. Engelbrecht, A., *Angew. Chem. Int. Ed. Engl.* **4,** 641 (1965).
5. Walton, R. A., *Prog. Inorg. Chem.* **16,** 1 (1972).
6. Gillespie, R. J., *Acc. Chem. Res.* **1,** 202 (1968).
7. Olah, G. A., and Olah, J. A., *in* "Carbonium Ions" (G. A. Olah and P. von R. Schleyer, Eds.), Vol. II, Chap. 17. Wiley, New York, 1970.
8. Farcasiu, D., *Acc. Chem. Res.* **15,** 46 (1982).
9. Pines, H., and Hoffman, N. E., *in* "Friedel-Crafts and Related Reactions" (G. A. Olah, Ed.), Vol. II, Part 2, Chap. 28. Wiley, New York, 1964.
10. Larsen, J. W., *J. Amer. Chem. Soc.* **99,** 4379 (1977).
11. Brilmyer, G., and Jasinski, R., *J. Electrochem. Soc.* **129,** 1950 (1982).
12. Siskin, M., Schlosberg, R. H., and Kocsi, W. P., *ACS Symp. Ser.* **55,** 186 (1977).
13. Fuentes, G. A., Boegel, J. V., and Gates, B. C., *J. Catal.* **78,** 436 (1982).
14. Hattori, H., Takahashi, O., Takagi, M., and Tanabe, K., *J. Catal.* **68,** 132 (1981).
15. Dooley, K. M., and Gates, B. C., *J. Polym. Sci. Polym. Chem.* **22,** 2859 (1984).
16. Dooley, K. M., Ph.D. thesis. University of Delaware, 1983.
17. Magnotta, V. L., and Gates, B. C., *J. Polym. Sci. Polym. Chem.* **15,** 1341 (1977).
18. Fuentes, G. A., and Gates, B. C., *J. Catal.* **76,** 440 (1982).
19. Crathorne, E. A., Howell, I. V., and Pitkethly, R. C., U.S. Patent 3,975,299 (1976).
20. McVicker, G. B., Kramer, G. M., Ziemiak, J. J., *J. Catal.* **83,** 323 (1983).
21. Krzywicki, A., and Marczewski, M., *J. Chem. Soc. Faraday* **76,** 1311 (1980).
22. Benesi, H. A., and Winquist, B. H. C., "Advances in Catalysis," Vol. 27, p. 97. Academic Press, New York, 1978.
23. Olah, G. A., "Friedel-Crafts Chemistry," Chap. 5. Wiley, New York, 1973.
24. Ono, Y., Tanabe, T., and Kitajima, N., *Chem. Lett.*, 625 (1978).
25. Olah, G. A., Surya Prakesh, G. K., and Sommer, J., *Science (Washington, D.C.)* **206,** 13 (1979).
26. Gillespie, R. J., and Peel, T. E., *J. Amer. Chem. Soc.* **95,** 5173 (1973).
27. Vinnik, M. I., Manelis, G. B., and Chirkov, N. M., *Russ. J. Inorg. Chem.* **2,** 306 (1957).
28. Kramer, G. M., *J. Org. Chem.* **40,** 298, 302 (1975).
29. Bernard, J. R., Brunel, D. E., Commeyras, A. A., Coste, C. M., Itier, J. J., and Knoche, H. W., U.S. Patent 3,960,764 (1976).
30. Rodewald, P. G., U.S. Patent 3,962,133 (1976).
31. Huang, T. J., and Yurchak, S., U.S. Patent 3,855,342 (1974).
32. Tanabe, K., and Hattori, H., *Chem. Lett.*, 625 (1976).